Observation and Calculation of Internal Structure in Scanning Tunneling Microscopy Images of Related Molecules

V. M. Hallmark and S. Chiang
IBM Research Division, Almaden Research Center, 650 Harry Road, San Jose, California 95120-6099

K.-P. Meinhardt and K. Hafner
Institut für Organische Chemie, Technical Hochschule Darmstadt, Darmstadt, Germany
(Received 27 January 1993)

The scanning tunneling microscope has been used to distinguish among a series of related molecules on Pt(111) by details of their observed structures. The electronic isomers naphthalene and azulene can be recognized, as can three structural isomers of monomethylazulene, as well as dimethyl- and trimethylazulene. The number and position of substituents affect the diffusion rates, sticking coefficients, and orientations. A simple methodology based on extended Hückel theory, including the substrate, generates electron and hole density plots which show very good agreement with the data.

PACS numbers: 61.16.Ch, 31.20.Pv, 68.35.Bs, 82.65.My

Chemisorbed molecules on surfaces are relevant to many chemical processes, including catalysis, corrosion, and etching. The ability to view such processes on an atomic scale in real time promises great progress in understanding and improving these processes. The development of the scanning tunneling microscope (STM) has now made possible the imaging of molecules on surfaces with near-atomic resolution [1] enabling, for example, studies of adsorbate organization [2] and analysis of internal molecular structure [3]. Real-space observation of surface reactions has already been achieved for simple systems such as the dissociation of ammonia on Si(111) [4], the oxidation of Cu(110) [5], and the conversion of ethylene to ethylidyne on Pt(111) [6]. More complex molecular reactions, however, will require an improved ability to distinguish subtle features of the adsorbate images in order to identify reactants, intermediates, and products. We have imaged a series of related molecules on Pt(111), including naphthalene, azulene, and a variety of methyl-substituted azulenes, to demonstrate the efficacy of the STM for recognizing individual species and for distinguishing among molecular isomers in mixed overlayers. These systematic observations have also assisted development of an image computation procedure based on extended Hückel theory (EHT). The extremely good agreement between calculated and observed images indicates that this computational method can provide a predictive tool for STM molecular imaging. Analysis of the computed images suggests that the STM probes electronic states formed by mixing molecular and metal states near the Fermi level.

The multichamber ultrahigh vacuum STM apparatus has been previously described in detail [7]. The Pt(111) crystal was cleaned by Ar-ion bombardment (500 eV) and flash annealed to 850 °C. The sample was generally cooled for 45 min to 1 h to allow the sample to equilibrate to room temperature. Molecules were dosed through a leak valve from a gas manifold heated to maintain the molecular vapor pressure near 1 torr. Further details of sample preparation are given elsewhere [2,8]. The constant current STM measurements were mostly performed with positive sample bias, ranging from 0.05 to 1.5 V, with tunneling currents of 0.5–4 nA, and with typical image acquisition times of 5–10 min. Low and high resolution molecular corrugations were approximately 1 and 2 Å, respectively. Atomic resolution on the Pt substrate was difficult to obtain and appears to require special tips which were unable to provide molecular resolution. Image processing usually consisted solely of background plane subtraction, although corrections for thermal drift and piezoelectric creep were made in Figs. 1 and 2.

Calculations of lowest unoccupied molecular orbitals (LUMO's) and highest occupied molecular orbitals (HOMO's) for isolated molecules have previously given good agreement with STM images for certain molecular systems [3,9]. Specific inclusion of the substrate, however, was required to reproduce details in the STM images

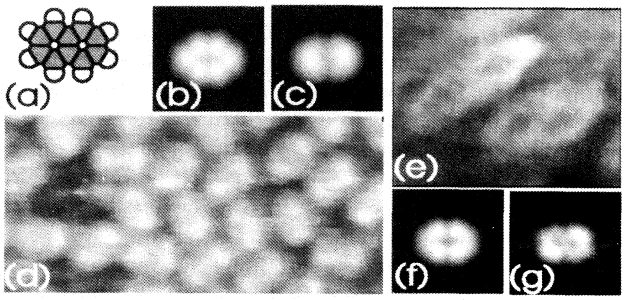

FIG. 1. Naphthalene on Pt(111). (a) Schematic of isolated molecule. (b) LUMO for isolated molecule, 2 Å above molecular plane. (c) ρ_H at 2 Å. (d) Low resolution STM image; the molecular van der Waals length is 8.1 Å. (e) High resolution STM image. (f) LUMO for isolated molecule, 0.5 Å above molecular plane. (g) ρ_H at 0.5 Å.

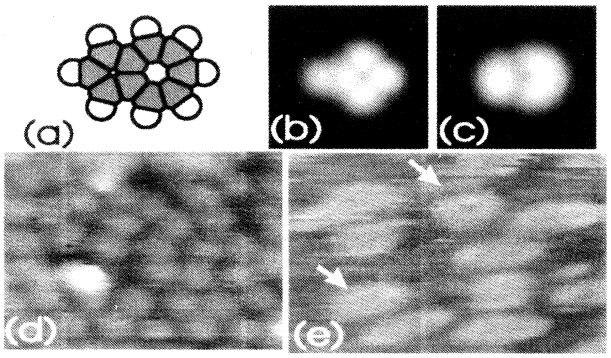

FIG. 2. Azulene on Pt(111). (a) Schematic of isolated molecule. (b) LUMO for isolated molecule, 2 Å above molecular plane. (c) ρ_H at 2 Å. (d) Low resolution STM image of near monolayer coverage azulene; molecular spacing within a (3×3) domain [8] is 8.3 Å. (e) High resolution STM image of mixed molecular overlayer, showing two azulenes (marked by arrows) among naphthalene neighbors.

reported here. The calculational procedure described below was optimized for naphthalene and then used without modification for the other molecular systems. In this sense, the predictive capabilities of the technique were tested against experimental observations. Explicit effects of various computational parameters will be reported in a future publication [10].

Since experimental data were similar for localized isolated molecules and close-packed molecules, images were calculated [11] only for single molecules. Each molecule was adsorbed with the ring system parallel to a single-layer Pt(111) cluster of thirteen atoms, although the effects of larger clusters and additional substrate layers have been explored. The energy of the system was minimized as a function of the adsorbate-metal separation for a variety of molecular binding sites and adsorbate orientations. Similar calculations of binding energy curves allowed predictions of molecular orientation, binding site, and relative diffusion rates for naphthalene and azulene on Pt(111) [12]; these predictions have now been verified by STM [2,8]. At minimum energy separation, the magnitude of the electron density for occupied states, or of the hole density for unoccupied states, at a given height above the plane of the molecule was calculated. As the number of metal atoms in the cluster increases, the population of metal states near the Fermi energy E_F also increases, and more mixing of molecular and metal states occurs. While certain states may dominate the electron or hole density near E_F at a particular height, these states may not be the LUMO or HOMO of the system, and such states may be separated from E_F by an increasing number of predominantly metal states. Analysis of the molecular contribution to states near E_F reveals that, while more metal states may be introduced, the energy of the dominant molecular state(s) stays constant. For this reason, we have introduced consistency among the systems studied by summing over all orbitals within a given energy range, either 1 V above or below E_F. These images have been convolved with a Gaussian of 1 Å width to simulate the effects of a finite tunneling tip. The result of this procedure is analogous to the ρ calculated by the STM theory of Tersoff and Hamann [13], with energy broadening due to a nonpoint probe. To facilitate comparisons with topography images, where the tunneling current decreases exponentially with distance, base 10 logarithmic plots of the resulting integrated electron density ρ_E, or hole density ρ_H, at a constant height are shown. The terms LUMO and HOMO in the following discussion should be understood to refer to the isolated molecule calculation.

The systems of naphthalene and azulene on Pt(111) have each been studied previously, using the techniques of low energy electron diffraction [14], thermal desorption spectroscopy, and STM [2,8]. Here we discuss only the molecular electronic structures imaged by STM and compare them with the calculations. Figure 1 gives both calculated and experimental STM images of naphthalene on Pt(111). Although the LUMO of Fig. 1(b) is clearly elongated, the pronounced bilobed structure typically observed for naphthalene, Fig. 1(d), is not apparent. For naphthalene in the on-top site with the long axis aligned with $[1\bar{1}0]$, as previously assigned by detailed molecular mapping of STM images onto Pt (3×3) lattices [2], ρ_H reproduces this bilobed structure quite clearly, as shown in Fig. 1(c). STM resolution is highly tip dependent, so that occasionally ultrahigh resolution is possible at lower tip-sample separation, such as in Fig. 1(e), where the double ring structure of naphthalene is explicitly observed. The effect of such higher resolution can be simulated by plots at a lower height. While the LUMO in Fig. 1(f) has no intensity in the bridge bond between the two rings, ρ_H in Fig. 1(g) correctly yields the double-ring structure.

Azulene, in comparison to naphthalene, diffuses rapidly on the surface at room temperature, and it is therefore difficult to obtain stable images at low coverage [8]. At approximately one monolayer coverage, (3×3) domains of azulene constrain the molecules sufficiently to allow molecular imaging, with the molecules appearing as indistinct round features [Fig. 2(d)]. Azulene can also be localized when coadsorbed with naphthalene, which appears to chemisorb more strongly to the Pt substrate. The three equivalent orientations and obvious double-ring structure of naphthalene in high resolution images of such mixed overlayers [Fig. 2(e)] confirm that the lack of elongation for azulene is not attributable to tip effects, but must be an inherent feature of the azulene adsorbate. Although azulene appears as a single ring, no obvious orientation of the molecule on the surface is manifested. Unlike naphthalene, azulene appears to translate and rotate freely at room temperature, so that the structural features of the calculations cannot be rigorously tested; rotation of both LUMO [Fig. 2(b)] and ρ_H [Fig. 2(c)]

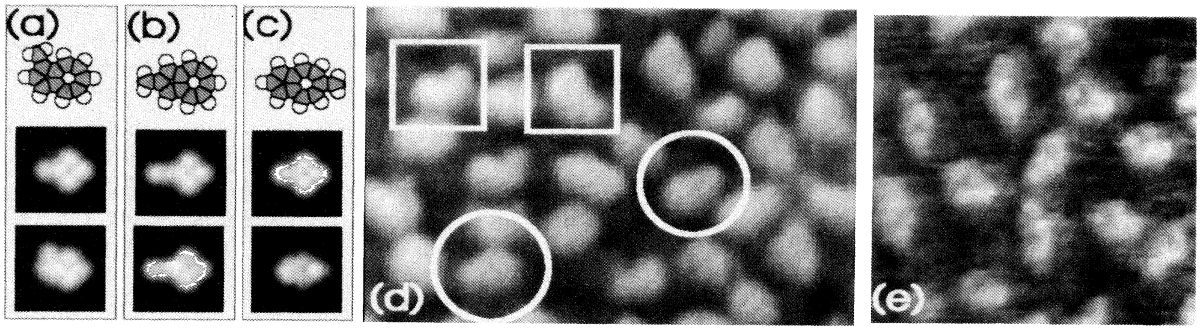

FIG. 3. Monomethylazulenes on Pt(111). Schematic, LUMO for isolated molecule (upper plot) and ρ_h (lower plot) for (a) 1-methylazulene (1-MA), (b) 2-MA, and (c) 6-MA. Plots for 1-MA and 2-MA are at 2 Å height, while that for 6-MA is at 0.5 Å height. (d) Low resolution STM image of mixed 1-MA, ~20% coverage [8] (in squares, e.g.), and 2-MA (in circles, e.g.) near saturation coverage. Some molecules appear to be impurity naphthalene or azulene or in motion. (e) High resolution STM image of 6-MA.

plots would lead to single ring structures.

Three different isomers of monomethylazulene (MA) provide a critical test, both of the ability of the STM to distinguish among similar molecules and of the predictive power of the computational method. All three isomers are distinguishable in STM images. The position of the methyl group can be identified from the molecular shapes [Figs. 3(d) and 3(e)]: 1-MA has a kidney-bean shape, 2-MA appears pearlike, and 6-MA (synthesis previously described [15]) has a diamond shape in low resolution images (not shown), while the hole in the seven-carbon ring is resolved in high resolution images. As shown in Figs. 3(a) and 3(c), the LUMO's for 1- and 6-MA are almost indistinguishable from each other, and from unsubstituted azulene [Fig. 2(b)]. The LUMO for 2-MA [Fig. 3(b)] is different in that it shows notable localized intensity at the methyl substitution site. In ρ_H plots for on-top sites, however, the methyl position on the ring is evident for all three MA's [Figs. 3(a)–3(c)]. The orientation of 2-MA has been assigned to be along $[1\bar{2}1]$ by direct comparison with that of naphthalene in mixed overlayers [8]. The orientation of 1-MA is assumed to be the same, although its resolution in images such as Fig. 3(d) is insufficient to mark the long axis of the azulene portion of the molecule. Since Figs. 3(d) and 3(e) have identical substrate orientation, comparison of observed axis directions for 2-MA and 6-MA allows the assignment of 6-MA along $[1\bar{1}0]$. For these MA cases, energy minimization revealed degeneracies for two orientations, but those orientations which correspond to the experimentally assigned ones yield better fits to the STM images.

Analysis of the isolated molecule and mixed molecule/metal orbitals for the case of 1-MA, for example, provides insight to the effect of the metal cluster on ρ_H. In contrast to the LUMO shown in Fig. 3(a), the HOMO clearly possesses intensity at the methyl site. Bonding with the metal cluster effectively mixes the HOMO and LUMO, which are the only two molecular states near E_F, so that the methyl group appears in both ρ_E and ρ_H plots. The ρ_E plot (not shown) is quite similar to the ρ_H plot, in agreement with the comparable experimental images at positive and negative bias.

Finally, synthesized 4,6,8-trimethylazulene [16] (TMA) [Fig. 4(c)] and 4,8-dimethylazulene [17] (DMA) [Fig. 4(d)] appear as clover-leaf structures in low resolution STM images, with a single bright spot appearing on one lobe of the molecule in many images. The LUMO's [Figs. 4(a) and 4(b)] reproduce this fourfold structure, but incorrectly predict that the methyl group at the end (6-) position would have higher intensity than the rest of the molecule in TMA and that DMA should not have a similar high intensity area. For consistency with the other plots shown here, ρ_H plots [Figs. 4(a) and 4(b)] are given for a Pt_{13} cluster, which is comparable to the molecular size for these larger adsorbates. ρ_H [Fig. 4(a)]

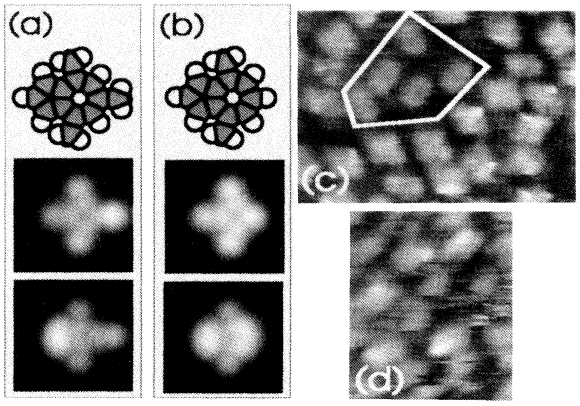

FIG. 4. Schematic, LUMO for isolated molecule (upper plot) and ρ_H (lower plot) for (a) 4,6,8-trimethylazulene and (b) 4,8-dimethylazulene. (c) STM image for mixed trimethylazulene and naphthalene (inside marked area) overlayer. (d) STM image for dimethylazulene at less than full coverage; noisy areas indicate molecules which move during the scan duration.

agrees with the experimental data for TMA by predicting that the molecular image should carry higher intensity on one lobe, the five-carbon ring. For DMA, although ρ_H [Fig. 4(b)] shows two lobes of comparable intensity, larger clusters provide a better fit with experimental data, showing higher intensity over the five-carbon ring. For these computations, both DMA and TMA have been placed in on-top sites, with the long-axis of the molecule aligned with [1$\bar{1}$0]. This orientation is deduced by comparison with that of naphthalene in mixed overlayers [Fig. 4(c)].

The systematic observation of this series of related molecules allows us to make comparisons of other molecular characteristics on the Pt(111) surface. We find that methyl substitution affects the apparent translational diffusion rates, as measured by relative motion of molecules during STM imaging, which increases in the following order: TMA, naphthalene, 6-MA, 2-MA, 1-MA, DMA, azulene [18]. Clearly, substitution position and number are both important in determining the adsorbate mobility. The sticking coefficients to the Pt surface can be inferred from the molecular dosing rates and the resulting molecular coverage on the surface in the STM images. The ordering of molecular sticking coefficients from high to low is as follows: naphthalene, TMA, 2-MA, 1-MA, azulene. These measurements seem to indicate an inverse relative relation between sticking coefficient and surface diffusion.

In conclusion, our systematic STM study of a series of related molecules has elucidated the capabilities of the instrument for molecular identification. In images with sufficiently high resolution, each molecule is readily distinguishable on the Pt(111) surface from details of its observed structure and surface diffusion. We have demonstrated, by comparison with this range of experimental data, that our calculational technique based on extended Hückel molecular orbital theory for the molecule/metal system adequately predicts details of internal structure. Our methodology has been shown to be superior to calculations involving only isolated molecule LUMO's and HOMO's. This technique should apply to other molecule-substrate systems and should allow correlation of internal features of the molecules with observed tunneling intensity. Despite the simplicity of the computation, qualitative features deduced by this method are comparable with those given by more advanced techniques, such as the elegant electron scattering methods used previously for STM image calculations [19]. For example, the observed threefold symmetry for benzene adsorbed on Rh(111) is easily obtained by our calculations, with benzene adsorbed in the threefold hollow site indicated by both LEED and STM measurements [20]. For the molecular systems described here, we have demonstrated semiquantitative analysis of the surface composition of mixed molecular monolayers from STM images, suggesting that identification and analysis of unknown adsorbates on a surface may be possible by these techniques in the future. Thus, these experiments and calculations together bring us closer to the goal of being able to observe more complicated chemical reactions on an atomic scale with the STM.

We would like to acknowledge useful discussions with J. K. Brown, K. E. Johnson, L. Haüssling, P. Sautet, and Ch. Wöll.

[1] S. Chiang, in *Scanning Tunneling Microscopy I,* edited by H.-J. Guntherodt and R. Wiesendanger (Springer-Verlag, Berlin, 1992), pp. 181–205.
[2] V. M. Hallmark, S. Chiang, J. K. Brown, and Ch. Woell, Phys. Rev. Lett. **66**, 48 (1991).
[3] P. H. Lippel, R. J. Wilson, M. D. Miller, Ch. Woell, and S. Chiang, Phys. Rev. Lett. **62**, 171 (1989).
[4] R. J. Hamers, Ph. Avouris, and F. Bozso, Phys. Rev. Lett. **59**, 2071 (1987).
[5] F. Besenbacher, F. Jensen, E. Laegsgaard, K. Mortensen, and I. Stensgaard, J. Vac. Sci. Technol. B **9**, 874 (1991).
[6] T. A. Land, T. Michely, R. J. Behm, J. C. Hemminger, and G. Comsa, Appl. Phys. A **53**, 414 (1991).
[7] S. Chiang, R. J. Wilson, Ch. Gerber, and V. M. Hallmark, J. Vac. Sci. Technol. A **6**, 386 (1988).
[8] V. M. Hallmark and S. Chiang, Surf. Sci. (to be published).
[9] D. P. E. Smith, J. K. H. Hörber, G. Binnig, and H. Nijoh, Nature (London) **344**, 641 (1990).
[10] V. M. Hallmark and S. Chiang (to be published).
[11] All EHT calculations were performed with FORTICON8 from Quantum Chemistry Program Exchange, using published Pt Hückel parameters from A. Gavezotti and M. Simonetta, Surf. Sci. **9**, 453 (1980).
[12] A. Gavezotti, E. Ortoleva, and M. Simonetta, Chem. Phys. Lett. **98**, 536 (1983).
[13] J. Tersoff and D. R. Hamann, Phys. Rev. Lett. **50**, 1998 (1983).
[14] D. Dahlgren and J. C. Hemminger, Surf. Sci. **109**, L513 (1981); **114**, 459 (1982), and references therein.
[15] K. Hafner and K.-D. Asmus, Liebigs Ann. Chem. **671**, 31 (1964).
[16] K. Hafner and H. Kaiser, Liebigs Ann. Chem. **618**, 140 (1958); Org. Synth. Coll. **5**, 1088 (1964).
[17] K. Hafner and H. Weldes, Liebigs Ann. Chem. **606**, 90 (1957).
[18] V. M. Hallmark, S. Chiang, K.-P. Meinhardt, and K. Hafner (to be published).
[19] P. Sautet and C. Joachim, Chem. Phys. Lett. **185**, 23 (1991); Surf. Sci. **271**, 387 (1992).
[20] H. Ohtani, R. J. Wilson, S. Chiang, and C. M. Mate, Phys. Rev. Lett. **60**, 2398 (1988).

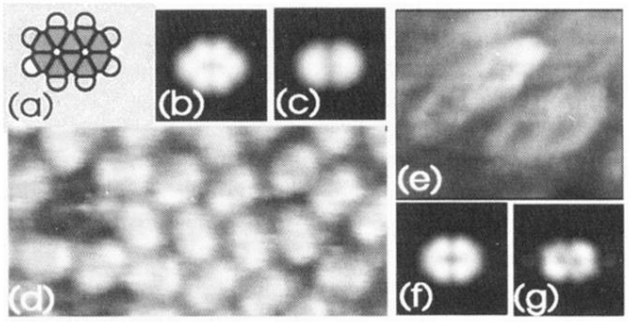

FIG. 1. Naphthalene on Pt(111). (a) Schematic of isolated molecule. (b) LUMO for isolated molecule, 2 Å above molecular plane. (c) ρ_H at 2 Å. (d) Low resolution STM image; the molecular van der Waals length is 8.1 Å. (e) High resolution STM image. (f) LUMO for isolated molecule, 0.5 Å above molecular plane. (g) ρ_H at 0.5 Å.

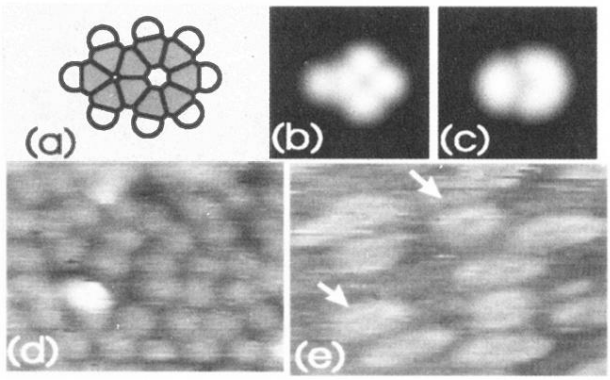

FIG. 2. Azulene on Pt(111). (a) Schematic of isolated molecule. (b) LUMO for isolated molecule, 2 Å above molecular plane. (c) ρ_H at 2 Å. (d) Low resolution STM image of near monolayer coverage azulene; molecular spacing within a (3×3) domain [8] is 8.3 Å. (e) High resolution STM image of mixed molecular overlayer, showing two azulenes (marked by arrows) among naphthalene neighbors.

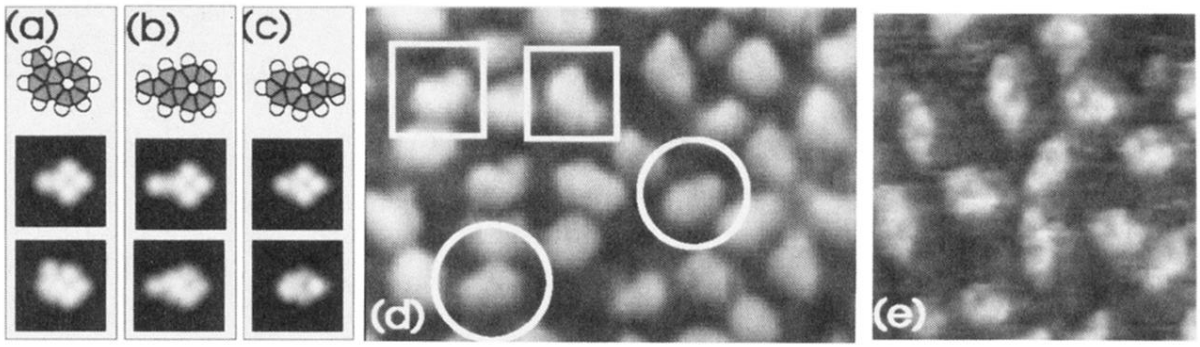

FIG. 3. Monomethylazulenes on Pt(111). Schematic, LUMO for isolated molecule (upper plot) and ρ_h (lower plot) for (a) 1-methylazulene (1-MA), (b) 2-MA, and (c) 6-MA. Plots for 1-MA and 2-MA are at 2 Å height, while that for 6-MA is at 0.5 Å height. (d) Low resolution STM image of mixed 1-MA, ~20% coverage [8] (in squares, e.g.), and 2-MA (in circles, e.g.) near saturation coverage. Some molecules appear to be impurity naphthalene or azulene or in motion. (e) High resolution STM image of 6-MA.

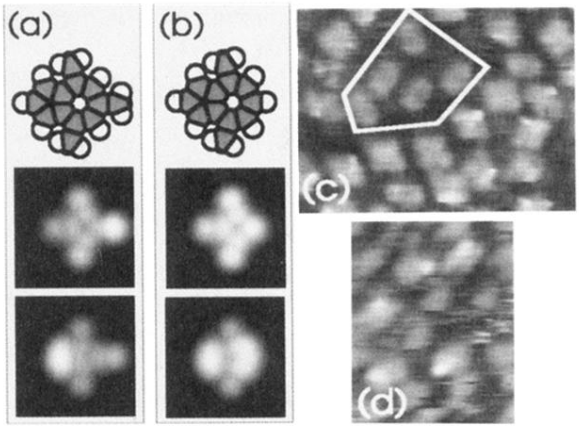

FIG. 4. Schematic, LUMO for isolated molecule (upper plot) and ρ_H (lower plot) for (a) 4,6,8-trimethylazulene and (b) 4,8-dimethylazulene. (c) STM image for mixed trimethylazulene and naphthalene (inside marked area) overlayer. (d) STM image for dimethylazulene at less than full coverage; noisy areas indicate molecules which move during the scan duration.